Dynamic gain-scheduled control of the ICE 101-TV

C. D. C. Jones, T. S. Richardson and M. H. Lowenberg
Department of Aerospace Engineering
University of Bristol, UK

ABSTRACT

This paper shows the theoretical development and application of dynamic gain scheduled control – a novel method for the control of nonlinear systems – to an aircraft model. The idea behind this method is to schedule the control law gains with a fast varying state variable rather than with a slow varying state or an input parameter. This is advantageous as it is then possible to schedule the gains with a state variable that is dominant in the mode that we are most interested in controlling. The use of this type of gain scheduling is shown to improve the transient response of the aircraft model when stepping between trim conditions and to overcome some of the problems associated with conventional gain scheduled controllers (such as control surface position limit saturation). 'Hidden coupling terms' that introduce unwanted dynamics when scheduling gains with a fast state (rather than the input design parameter) are eliminated directly by applying a transformation to the classical parameter-scheduled gain distributions which are calculated using eigenstructure assignment. A second order longitudinal model and a 5th order longitudinal/lateral model of the ICE 101-TV tailless delta-wing aircraft configuration are used to demonstrate the design process.

NOMENCLATURE

Symbols

$C_{M\alpha}$	pitch stiffness coefficient
C_N	normal force coefficient
k_i	mass moment of inertia term
K	static gain
L	body axis rolling moment
m	aircraft mass
M	body axis pitching moment
N	body axis yawing moment
p	body axis roll rate
q	body axis pitch rate
q_{dem}	demanded body axis pitch rate
q_{int}	q CAS integrator state
r	body axis yaw rate
$\bar{r}$	reference input
$\mathbf{u}$	control input vector
$\mathbf{u_0}$	control input vector at equilibrium point
$\mathbf{V}$	modal matrix of achievable eigenvectors
V_T	total translational velocity
$\mathbf{x}$	state vector
$\mathbf{x_0}$	state vector at equilibrium point
x_E	x-earth axis co-ordinate of the aircraft body axes origin
y_E	y-earth axis co-ordinate of the aircraft body axes origin
Y_W	y-wind axis aerodynamic force
z_E	z-earth axis co-ordinate of the aircraft body axes origin
Z_W	z-wind axis aerodynamic force

Abbreviations

AMT	all-moving tip
AMTact	all-moving tip actuator
AMTL	all-moving tip (left)
AMTLact	all-moving tip (left) actuator

Paper No. 2947. Manuscript received 17 December 2004, revised version received 26 July 2005, accepted 26 August 2005.

https://doi.org/10.1017/S0001924000000932 Published online by Cambridge University Press

AMTR	all-moving tip (right)
AMTRact	all-moving tip (right) actuator
CAS	command augmentation system
CG	centre of gravity
DGS	dynamic gain schedule
ELEV	elevon
F-DGS	full dynamic gain schedule
ICE	innovative control effectors
LEF	leading-edge flap
M-DGS	modified dynamic gain schedule
PF	pitch flap
PFact	pitch flap actuator
SAS	stability augmentation system
SCAS	stability and command augmentation system
SPLR	spoiler
SSD	spoiler slot deflector
UCAV	unmanned combat air vehicle

Greek symbols

α	angle of incidence
β	angle of sideslip
β_{dem}	demanded angle of sideslip
β_{int}	β CAS integrator state
δ_e	elevator actuator position
$\delta_{e\ dem}$	demanded elevator actuator position
$\delta_{yaw}act$	yaw thrust vectoring actuator
φ	dynamic gain
$\mathbf{\Lambda}$	matrix of desired eigenvalues
μ	continuation parameter
μ_0	continuation parameter at equilibrium point
ρ	density of air
θ	pitch attitude
ψ	heading angle
v_i^d	desired eigenvector

1.0 INTRODUCTION

Gain scheduling has been described as the process of subdividing a nonlinear control problem into a series of linear ones, design of controllers to suit each linear design condition and then reconstruction of the resultant set of gains into a single continuous controller[1]. There has been an upsurge in gain-scheduling research in the last decade[2-8]. The aim of this work has been to relax the restrictions associated with classical gain-scheduling approaches, in particular (according to Ref. 9):

- the restriction to near equilibrium operation that arises from the use of only equilibrium information (namely, the equilibrium linearisations of the plant) for control design purposes.
- the slow variation conditions associated with ensuring that the overall system does not evolve between operating regions in too rapid a manner.

The former of these restrictions can be addressed using representations based on fuzzy/neural approaches, linear/quasi-linear parameter-varying formulations and off-equilibrium linearisation[9]. (It should be noted that this restriction is not particular to gain-scheduling but applies to linear models in general.) However, the relaxation of the latter restriction is still an open question. This paper focuses on addressing this latter restriction by using dynamic state-feedback gain scheduling which has been defined in Ref. 1:

"…scheduling gains with one (or more) of the system states whilst accounting for the 'hidden coupling terms' ensures that the controller gains are always set for the current state space location and therefore produce a near-optimal response."

This type of controller is particularly useful when large control inputs are demanded rapidly. These could occur when a pilot is carrying out an evasive manoeuvre or when the higher level mission controller of a semi-autonomous unmanned combat air vehicle (UCAV) requires a sudden change in trajectory.

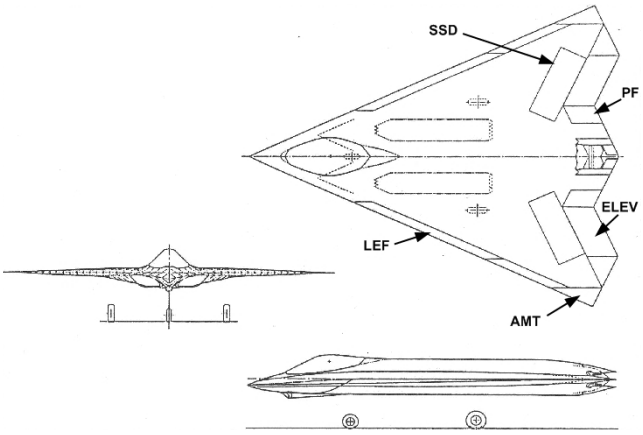


Figure 1. Schematic drawing of the ICE[10].

In this work the method is applied to a highly non-linear aircraft model, the ICE 101-TV[10,11], which was designed by Lockheed Martin Tactical Aircraft Systems as part of the innovative control effectors (ICE) programme. It is a tailless delta-wing configuration with a 65° leading-edge sweep and a sawtooth trailing edge. It has five aerodynamic control surfaces as shown in Fig. 1 – all-moving wing tips (AMT), pitch flaps (PF), leading edge flaps (LEF), elevons (ELEV), spoiler slot deflectors (SSD) – and a pitch/yaw thrust vectoring capability. Although the ICE was not specifically designed to be unmanned, its configuration is similar to some current UCAVs[12] and is therefore suitable for unmanned research studies.

Results are presented for a second order longitudinal model with a q-demand (q_{dem}) stability and command augmentation system (SCAS) and for a fifth order longitudinal/lateral model with a β-demand (β_{dem}) SCAS. The static gains are determined iteratively from within a continuation design framework[13] using eigenstructure assignment. This has the advantage of giving the user an explicit knowledge of the closed-loop dynamics throughout parameter space and a strong link with the underlying physics is retained. State-scheduled dynamic gains are then calculated directly from these parameter-scheduled static gains.

2.0 METHODOLOGY/PROBLEM DEFINITION

Following the methodology in Ref. 14, first consider the nonlinear system:

$$\dot{x} = F(x, \delta) \qquad \ldots (1)$$

where:
$\mathbf{x} \in \Re^n$ is the state vector
$\boldsymbol{\delta} \in \Re^p$ is a vector of parameters
$\mathbf{F} : \Re^{n+p} \rightarrow \Re^n$ is a nonlinear system

Fixing all elements in $\boldsymbol{\delta}$ apart from one, μ:

$$\dot{\mathbf{x}} = \boldsymbol{f}(\mathbf{x}, \mu) \qquad \ldots (2)$$

https://doi.org/10.1017/S0001924000000932 Published online by Cambridge University Press

where:

$f : \Re^{n+1} \rightarrow \Re^n$ is a nonlinear system and then adding a nonlinear controller gives the system:

$$\dot{x} = g(x, \mu, u) \quad \ldots (3)$$

where:
$\mathbf{u} \in \Re^m$ is a vector of control inputs
$\mathbf{g} : \Re^{n+1+m} \rightarrow \Re^n$ is a nonlinear system

With μ fixed, linearise about an equilibrium point (x_0, μ_0, u_0) to give:

$$\dot{\hat{x}} = A\hat{x} + B\hat{u} \quad \ldots (4)$$

where $\hat{x}$ and $\hat{u}$ are perturbations from the linearisation point; u is the sum of a feedforward signal, u_{ff}, and a feedback signal, ufb. Consider a positive state feedback scheme where u_{fb} is considered in terms of x and an appropriate feedback gain matrix, **K**, giving the closed loop system:

$$\dot{\hat{x}} = A\hat{x} + BK\hat{x} + B\hat{u}_{ff} = A_{cl}\hat{x} + B\hat{u}_{ff} \quad \ldots (5)$$

u_{ff} is assumed to be zero as it has no effect on the closed-loop stability. Hence Equation (5) reduces to:

$$\dot{\hat{x}} = A_{cl}\hat{x} \quad \ldots (6)$$

The gain matrix can then be calculated from the above linearization using, in this case, eigenstructure assignment[15-18] though other approaches such as H_∞ [19] or LQR[20,21] can also be used. This is done quasi-continuously at trim points throughout the μ range by incorporating the eigenstructure assignment process within a continuation algorithm (using the AUTO software[22], in this case); μ is defined as the continuation parameter.

2.1 Dynamic gain scheduling with the feedback state

The gain matrices can vary considerably between points in state-space for a highly nonlinear system so it is necessary to schedule them against either x or μ to maintain the desired control performance. Scheduling against x leads to a problem as demonstrated by the following simple example:

Let a second order aircraft system in α (the angle of incidence) and q (the pitch rate) with state feedback on both states be represented by the following equations of motion:

$$\begin{aligned} \dot{\alpha} &= f_1(\alpha, q) \\ \dot{q} &= f_2(\alpha, q) + K_\alpha(\bar{r})\alpha + K_q(\bar{r})q \end{aligned} \quad \ldots (7)$$

where $\bar{r}$ is the reference input which is equal to μ for all the cases considered in this paper. As an example, for an aircraft system $\bar{r}$ could be elevator angle, δ_e for an open-loop system, or pitch rate demand, q_{dem}, for a closed-loop system. In general μ can be any of the elements of δ, for example, centre of gravity position CG, mass m, elevator angle δ_e or pitch rate demand q_{dem}. Hence δ contains both the exogeneous reference signal, $\bar{r}$, and internal parameters.

The Jacobian, **J**, of this system has the form:

$$J = \begin{bmatrix} \frac{\partial \dot{\alpha}}{\partial \alpha} & \frac{\partial \dot{\alpha}}{\partial q} \\ \frac{\partial \dot{q}}{\partial \alpha} & \frac{\partial \dot{q}}{\partial q} \end{bmatrix} \quad \ldots (8)$$

If the gains are scheduled with $\bar{r}$ then the terms in **J** become:

$$\begin{aligned} \frac{\partial \dot{\alpha}}{\partial \alpha} &= \frac{\partial f_1}{\partial \alpha} \\ \frac{\partial \dot{\alpha}}{\partial q} &= \frac{\partial f_1}{\partial q} \\ \frac{\partial \dot{q}}{\partial \alpha} &= \frac{\partial f_2}{\partial \alpha} + K_\alpha(\bar{r}) \\ \frac{\partial \dot{q}}{\partial q} &= \frac{\partial f_2}{\partial q} + K_q(\bar{r}) \end{aligned} \quad \ldots (9)$$

If, however, each gain is scheduled with its feedback state instead of the reference input then the terms in **J** become:

$$\begin{aligned} \frac{\partial \dot{\alpha}}{\partial \alpha} &= \frac{\partial f_1}{\partial \alpha} \\ \frac{\partial \dot{\alpha}}{\partial q} &= \frac{\partial f_1}{\partial q} \\ \frac{\partial \dot{q}}{\partial \alpha} &= \frac{\partial f_2}{\partial \alpha} + K_\alpha(\alpha) + \frac{\partial K_\alpha}{\partial \alpha}\alpha \\ \frac{\partial \dot{q}}{\partial q} &= \frac{\partial f_2}{\partial q} + K_q(q) + \frac{\partial K_q}{\partial q}q \end{aligned} \quad \ldots (10)$$

The problem arises because when designing the controller, the gains are calculated at specific reference points, i.e. in a 'static' sense, $\partial K_\alpha/\partial_\alpha = \partial K_q/\partial q = 0$. When implemented, however, these partial derivatives are not in general zero since α and q are dynamically varying states of the system.

Hence, scheduling against the feedback state rather than with the reference input introduces coupling terms (between dependent and independent schedule variables) which produce unwanted additional dynamics. Our approach to minimising the effect of the coupling terms is to define a different set of gain schedules that retain the same eigenstructure as in the design (static) situation at all reference (trim) conditions.

Therefore, the problem associated with gain scheduling against a state, x, is to find a nonlinear gain matrix, $\varphi(x)$, such that the closed loop system has the same desired eigenstructure as a system that schedules its gains, $K(\bar{r})$, with $\bar{r}$. The solution to this problem is most simply explained by example by considering the following first order system:

$$\dot{x} = f(x, \mu) + u \quad \ldots (11)$$

where $x \in \Re$, $u \in \Re$. Assume we wish to design two controllers of the form $u = K(\bar{r})x$ and $u = \varphi(x)x$ by eigenstructure assignment of the linearised model about a set of trimmed points. It has been shown in Ref. 1 that if the eigenstructures of the two closed loop systems are to be identical then the two sets of gains $K(\bar{r})$ and $\varphi(x)$ are related by the following equation:

$$K(\bar{r}) = \frac{\partial \varphi}{\partial x}x + \varphi(x) \quad \ldots (12)$$

Therefore, the dynamic gain schedule (DGS) is given by:

$$\varphi(x) = \frac{\int K(\bar{r})\mathrm{d}x + c}{x} \quad \ldots (13)$$

where c is the constant of integration.

From this point onwards, if the gains are scheduled with either the reference input, $\bar{r}$, or a slowly-varying state then they will be referred to as static gains, K. Gains that have been transformed to allow scheduling with a fast-varying state will instead be referred to as dynamic gains. Hence the static gain schedule, K, is transformed to a dynamic gain schedule, φ, to improve its response to rapid

https://doi.org/10.1017/S0001924000000932 Published online by Cambridge University Press

control demands.

The transformation from static gain, K, to dynamic gain, φ, can be applied to any nth order system provided that each gain is only scheduled against the state to which it is applied. If there is such feedback on any state in any of the n equations then the transformation in Equation (13) can be used to find $\varphi(x)$ from $K(\bar{r})$. For example,

$$\dot{x}_1 = f(x) + K_1(\bar{r})x_1 + K_2(\bar{r})x_2 \quad \ldots (14)$$

can be used to get:

$$\dot{x}_1 = f(x) + \varphi_1(x_1)x_1 + \varphi_2(x_2)x_2 \quad \ldots (15)$$

In practice, φ is determined as follows:

$$\varphi(x_u)x_u = \int_{x_l}^{x_u} K(\bar{r})\mathrm{d}x + \varphi(x_l)x_l \quad \ldots (16)$$

where x_u and x_l are the upper and lower limits of x respectively.

Dynamic state-scheduled gains directly account for the coupling terms in the Jacobian matrix as the DGS is obtained by applying a transformation to the static gain schedule.

Therefore, for the system defined by Equation (7) the dynamic gains can be related to the static gains by simply applying Equation (12) in the following way:

$$\begin{aligned} K_q &= q\frac{\partial \varphi_q}{\partial q} + \varphi_q(q) \\ K_\alpha &= \alpha\frac{\partial \varphi_\alpha}{\partial \alpha} + \varphi_\alpha(\alpha) \end{aligned} \quad \ldots (17)$$

2.2 Dynamic gain scheduling with a state other than the feedback state

It is sometimes not possible to convert a static gain schedule to a DGS by simply applying Equation (13) due to the numerics of the data, e.g. when the function relating the states, x, to the gain, K, is not a one-to-one function ($y = \sqrt{x}$ would be an example of a one-to-many function). One of the advantages of the continuation-based approach is that the nature of K throughout parameter space will be immediately apparent.

In such situations it is possible to schedule with a state other than the feedback state but the DGS must then be calculated using an alternative transformation. This novel process will be defined as a 'modified' transformation and the resulting gain schedule as a modified dynamic gain schedule (M-DGS). It is best described by the following two examples:

1. Consider a third order closed-loop aircraft system (α, q, δ_e) where the elevator actuator transfer function relating its position, δ_e, to its demanded position, $\delta_{e_{dem}}$, is modelled as a first order lag:

$$\delta_e = \frac{30}{s+30}\delta_{e_{dem}} \quad \ldots (18)$$

Rearranging and taking inverse Laplace transforms gives:

$$\dot{\delta}_e = -30\delta_e + 30\delta_{e_{dem}} \quad \ldots (19)$$

If the reference input is zero and a positive feedback scheme is assumed with the gains scheduled with the input parameter, μ, then:

$$\dot{\delta}_e = -30\delta_e + 30[K_\alpha(\mu)\alpha + K_q(\mu)q] \quad \ldots (20)$$

Hence the system is defined as:

$$\begin{aligned} \dot{\alpha} &= f_1(\alpha, q, \delta_e) \\ \dot{q} &= f_2(\alpha, q, \delta_e) \\ \dot{\delta}_e &= -30\delta_e + 30[K_\alpha(\mu)\alpha + K_q(\mu)q] \end{aligned} \quad \ldots (21)$$

Now if state-scheduled dynamic gain feedback is required instead of μ-scheduled static gain feedback then the final line of Equation (21) is replaced by:

$$\delta_e = -30\delta_e + 30[\varphi_\alpha(\alpha)\alpha + \varphi_q(q)q] \quad \ldots (22)$$

and the standard transformations can be applied to get the dynamic gains, φ, from the static gains, K, which are in this case the same as those given in Equation (17).

However, if for example K_q can not be transformed to φ_q using q because of the numerics of the data then the $\dot{\delta}_e$ equation may take the following form instead:

$$\dot{\delta}_e = -30\delta_e + 30[\varphi_\alpha(\alpha)\alpha + \varphi_q(\alpha)q] \quad \ldots (23)$$

i.e. φ_q scheduled with α instead of q. By equating the elements of the Jacobian matrix of the μ-scheduled system to those of the state-scheduled system the transformation set becomes:

$$\begin{aligned} K_\alpha &= \varphi_\alpha(\alpha) + \frac{\partial \varphi_\alpha}{\partial \alpha}\alpha + \frac{\partial \varphi_q}{\partial \alpha}q \\ K_q &= \varphi_q(\alpha) \end{aligned} \quad \ldots (24)$$

It is then possible to find φ_α using Equation (13) because $\partial\varphi_q/\partial\alpha$ can be determined numerically as a result of the second relationship in Equation (24).

The benefits of this 'modified' transformation will depend on the system. In general, a better performing system than the parameter-scheduled one will result but an inferior response when compared to the conventional transformation is likely. The reason for this lies in the inherent smoothing performed by the transformation of a schedule from static to dynamic due to the integration of the static gain schedule with respect to the feedback state. This results in the magnitude of the feedback signal to the actuator at off-trim points being less than it would have been with the untransformed schedule, so actuator movement is reduced, leading to less significant transient motion. The modified transformation will smooth at least one less schedule than the conventional transformation hence the system gains, although scheduled with a fast state and having the desired eigenvalues, may retain many of their nonlinearities.

2. Consider a sixth order closed-loop aircraft system (α, β, p, q, r, δ_e):

$$\begin{aligned} \dot{\alpha} &= f_1(\alpha, \beta, p, q, r, \delta_e) \\ \dot{\beta} &= f_2(\alpha, \beta, p, q, r, \delta_e) \\ \dot{p} &= f_3(\alpha, \beta, p, q, r, \delta_e) \\ \dot{q} &= f_4(\alpha, \beta, p, q, r, \delta_e) \\ \dot{r} &= f_5(\alpha, \beta, p, q, r, \delta_e) \\ \dot{\delta}_e &= -30\delta_e + 30[K_\alpha(\mu)\alpha + K_\beta(\mu)\beta + K_p(\mu)p \\ &\quad + K_q(\mu)q + K_r(\mu)r] \end{aligned} \quad \ldots (25)$$

where β = angle of sideslip, p = body axis roll rate, and r = body axis yaw rate.

Now if state-scheduled dynamic gain feedback is required instead of μ-scheduled static gain feedback then Equation (25) is replaced by:

$$\dot{\delta}_e = -30\delta_e + 30[\varphi_\alpha(\alpha)\alpha + \varphi_\beta(\beta)\beta + \varphi_p(p)p + \varphi_q(q)q + \varphi_r(r)r] \quad \ldots (26)$$

https://doi.org/10.1017/S0001924000000932 Published online by Cambridge University Press

and the standard transformation can be applied to get the dynamic gains, φ, from the static gains, K:

$$\begin{aligned} K_\alpha &= \varphi_\alpha(\alpha) + \frac{\partial \varphi_\alpha}{\partial \alpha}\alpha \\ K_\beta &= \varphi_\beta(\beta) + \frac{\partial \varphi_\beta}{\partial \beta}\beta \\ K_p &= \varphi_p(p) + \frac{\partial \varphi_p}{\partial p}p \\ K_q &= \varphi_q(q) + \frac{\partial \varphi_q}{\partial q}q \\ K_r &= \varphi_r(r) + \frac{\partial \varphi_r}{\partial r}r \end{aligned} \quad \ldots (27)$$

However, if in the extreme case where all but one of the gains can not be transformed using their own state, then the δ_e equation may instead take the form:

$$\begin{aligned} \dot{\delta}_e = -30\delta_e + 30[&\varphi_\alpha(r)\alpha + \varphi_\beta(r)\beta + \varphi_p(r)p \\ &+ \varphi_q(r)q + \varphi_r(r)r] \end{aligned} \quad \ldots (28)$$

i.e. the gains are all scheduled with yaw rate, r, and the transformation set, by equating the elements of the Jacobian of the parameter-scheduled system to those of the state-scheduled system, becomes:

$$\begin{aligned} K_\alpha &= \varphi_\alpha(r) \\ K_\beta &= \varphi_\beta(r) \\ K_p &= \varphi_p(r) \\ K_q &= \varphi_q(r) \\ K_r &= \varphi_r(r) + \frac{\partial \varphi_r}{\partial r}r + \frac{\partial \varphi_q}{\partial r}q + \frac{\partial \varphi_p}{\partial r}p + \frac{\partial \varphi_\beta}{\partial r}\beta + \frac{\partial \varphi_\alpha}{\partial r}\alpha \end{aligned} \quad \ldots (29)$$

2.3 General result for the transformation of static to dynamic gain schedules

Therefore, for a system of the form:

$$\begin{aligned} \dot{x}_1 &= f_1(x_1 \ldots x_n) \\ \dot{x}_2 &= f_2(x_1 \ldots x_n) \\ &\vdots \\ \dot{x}_{n-1} &= f_{n-1}(x_1 \ldots x_n) \\ \dot{x}_n &= -30x_n + 30[K_1(\mu)x_1 + \cdots + K_{n-1}(\mu)x_{n-1}] \end{aligned} \quad \ldots (30)$$

The general transformation set is given by:

$$\begin{aligned} K_{a_i}(\mu) &= \varphi_{a_i}(a_i) + \frac{\partial \varphi_{a_i}}{\partial a_i}a_i + \sum_{j=1}^{b_n} a_{flag}\frac{\partial \varphi_{b_j}}{\partial a_i}b_j\Big|_{i=1,a_n} \\ K_{b_i}(\mu) &= \varphi_{b_i}(a_{aux_i})\Big|_{i=1,b_n} \end{aligned} \quad \ldots (31)$$

where:
$a \in \Re^{a_n}$ is the vector of feedback states that can be used to schedule the associated feedback gain;
$b \in \Re^{b_n}$ is the vector of the remaining feedback states;
$a_{aux} \in \Re^{b_n}$ is the vector of states against which φ_{b_i} is scheduled;
a_{flag} is defined as:

$$a_{flag} = \begin{cases} 1 & if\ a_i = a_{aux_j} \\ 0 & if\ a_i \neq a_{aux_j} \end{cases} \quad \ldots (32)$$

e.g. in the second example of Section 2.2: $a = [r]$, $b = [\alpha, \beta, p, q]$, $a_{aux} = [r, r, r, r]$.

3.0 RESULTS

DGS control is now assessed using two versions of the ICE. First, however, a brief description of the open-loop aircraft dynamics is presented.

3.1 Open-loop ICE model

The equations of motion of the fifth order open-loop ICE model are defined in the standard way:

$$\begin{aligned} \dot{\alpha} &= q - \mathrm{Tan}\beta(p\,\mathrm{Cos}\alpha + r\,\mathrm{Sin}\alpha) + \frac{Z_W}{mV_T\,\mathrm{Cos}\beta} \\ \dot{\beta} &= p\,\mathrm{Sin}\alpha - r\,\mathrm{Cos}\alpha + \frac{Y_W}{mV_T} \\ \dot{p} &= k_1 qr + k_2 pq + k_3 L + k_4 N \\ \dot{q} &= k_5 rp + k_6(r^2 - p^2) + k_7 M \\ \dot{r} &= k_8 pq + k_9 qr + k_4 L + k_{10} N \end{aligned}$$

where each state, variable and parameter takes their usual meaning (see Nomenclature) and the forces and moments are highly nonlinear functions of α, β and the effector deflections. For convenience the mass moment of inertias are written as:

$$k_1 = \frac{(I_{yy} - I_{zz})I_{zz} - I_{xz}^2}{I_{xx}I_{zz} - I_{xz}^2} \quad k_2 = \frac{(I_{xx} - I_{yy} + I_{zz})I_{xz}}{I_{xx}I_{zz} - I_{xz}^2} \quad \ldots (33)$$

$$k_3 = \frac{I_{zz}}{I_{xx}I_{zz} - I_{xz}^2} \quad k_4 = \frac{I_{xz}}{I_{xx}I_{zz} - I_{xz}^2} \quad k_5 = \frac{(I_{zz} - I_{xx})}{I_{yy}}$$

$$k_6 = \frac{I_{xz}}{I_{yy}} \quad k_7 = \frac{1}{I_{yy}} \quad k_8 = \frac{(I_{xx} - I_{yy})I_{xx} + I_{xz}^2}{I_{xx}I_{zz} - I_{xz}^2} \quad \ldots (34)$$

$$k_9 = \frac{(I_{yy} - I_{zz} - I_{xx})I_{xz}}{I_{xx}I_{zz} - I_{xz}^2} \quad k_{10} = \frac{I_{xx}}{I_{xx}I_{zz} - I_{xz}^2}$$

This reduced order model captures the dynamics of the fast aircraft modes i.e. the short period pitching oscillation, the Dutch roll and the roll subsidence mode. In this work, each analysis is carried out at V_T = 190ms^{-1} and at a nominal altitude of 20,000ft (Mach number = 0·6) with all the other states that conventionally define the aircraft dynamics θ, ψ, x_E, y_E (see Nomenclature) set to zero. Bank angle is also set to zero.

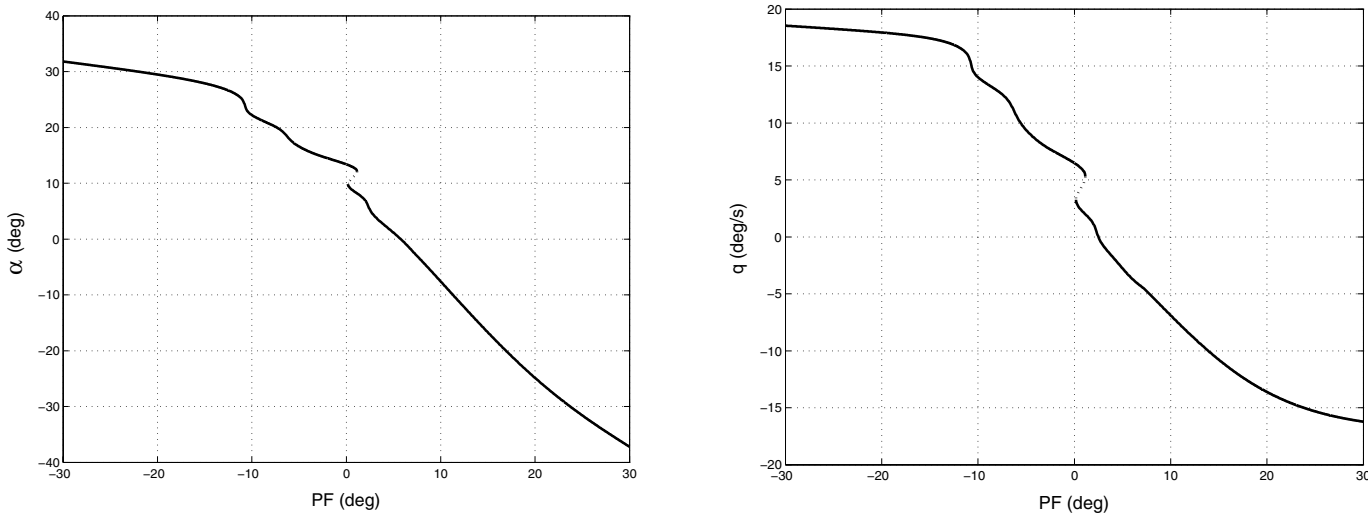
A second order (α, q) version of the model is also used (where β, p and r are fixed at 0) which enables analysis of the short period pitching oscillation alone.

An analysis of the open-loop models was carried out using the AUTO continuation software. Figure 2 shows the bifurcation diagrams[23-26] for the second order open-loop model with the pitch flap (PF) deflection as the continuation parameter (μ). Solid lines indicate stable branches while dotted lines indicate unstable branches. Hence the system is unstable in the region 10° < α < 12·5°. This is a result of positive pitch stiffness, $C_{M\alpha}$, in this region.

Figure 3 shows the bifurcation diagrams for the fifth order open-loop model with the pitch flap as the continuation parameter. There is a main 'trim' branch, two 'lateral' branches in the mid-α range (resulting from pitchfork bifurcations) and a high-α spin branch. Note that p, q and r are omitted for brevity. The additional unstable regions are caused by negative $C_{l\beta}$ and $C_{n\beta}$ which could be stabilised by adding dihedral to the wings and a vertical tail surface respectively (or by feedback control).

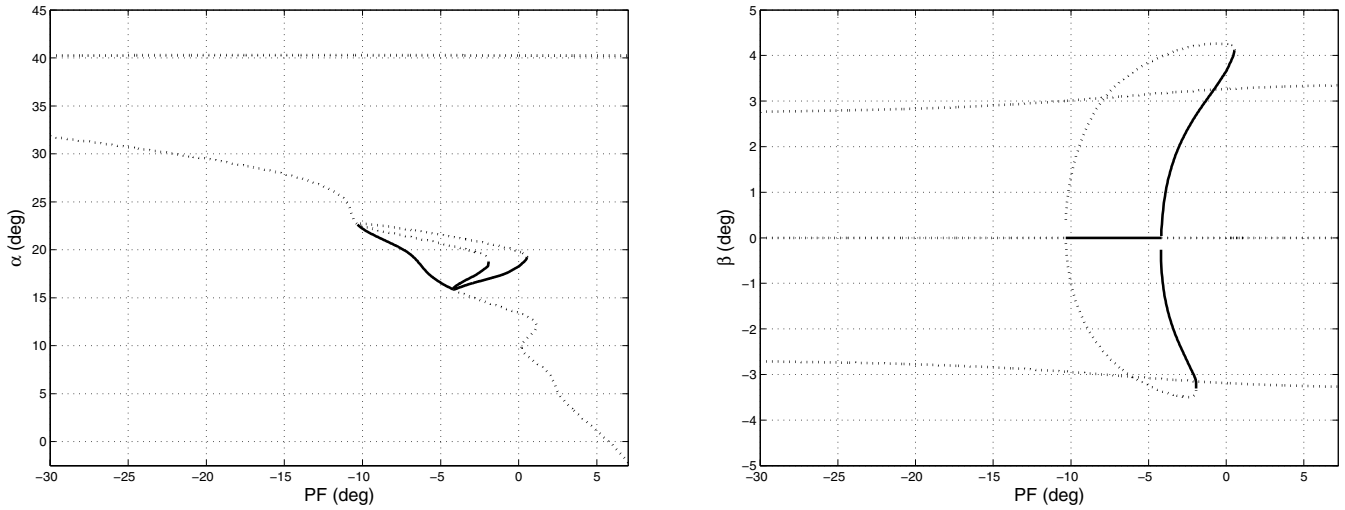
The asymmetries in the non-zero 'lateral' branches result from slightly asymmetric lateral force and moment coefficients. These asymmetries are caused by typical wind tunnel effects, e.g. flow angularity, slight model asymmetry, and sting bending. They grow

https://doi.org/10.1017/S0001924000000932 Published online by Cambridge University Press



(a) α (b) q

Figure 2. Open-loop bifurcation diagrams with μ = PF.



(a) α (b) β

Figure 3. Fifth order open-loop bifurcation diagrams with μ = PF.

with angle of attack due to typical asymmetric vortex effects. The result is a highly nonlinear aircraft model that presents a suitably complex control task to enable a rigorous assessment of this new control method. Figure 4 shows open-loop bifurcation diagrams with AMTL as the continuation parameter. The μ-limits are fairly narrow to make the folds clearer – beyond the plotted range a linear extrapolation of the state values gives a good approximation of the actual state values. Hence the AMTL is capable of providing substantial lateral and directional control power but the moments it produces for small deflections (less than 2 deg) are highly non-linear.

3.2 Closed-loop ICE model

The closed-loop systems analysed in the remainder of this paper have been given version numbers for ease of reference and are defined in Table 1. Each has a SCAS and the actuators have been modelled by simple first order lags of the form 30/(*s*+30) with position saturation limits only.

The closed-loop systems were incorporated into the AUTO continuation software with the static gains being calculated iteratively for each trim point using eigenstructure assignment. A brief summary of the eigenstructure assignment method of controller design follows which is based on the description given in Ref. (18):

For a linearised closed-loop system of the form:

$$\dot{\hat{x}} = A\hat{x} + BK\hat{x} \qquad \ldots (35)$$

the eigenvalues and eigenvectors are related to the closed loop state matrix by:

$$\mathbf{(A + BK)V = \Lambda V} \qquad \ldots (36)$$

where $\mathbf{\Lambda}$ is a matrix that has the closed-loop eigenvalues on the principle diagonal and the achievable closed-loop eigenvectors are given in the modal matrix, $\mathbf{V}$.

It is not possible to simply specify any set of eigenvalues and eigenvectors – this is dependent on the number of feedback states that are available and the number of control inputs. The number of

https://doi.org/10.1017/S0001924000000932 Published online by Cambridge University Press

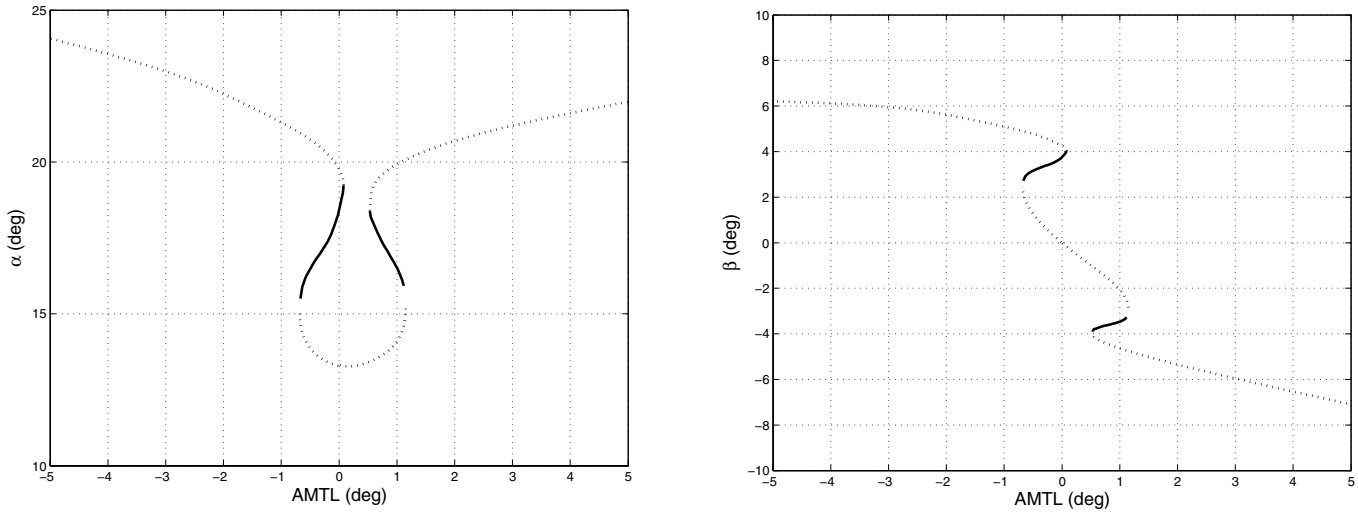


Figure 4. Fifth order open-loop bifurcation diagrams with μ = AMTL.

Table 1
ICE model version definitions

Version	Aircraft states	Actuators	CAS	Model order
v1	α, q	PF	q_{dem}	4th
v2	α, β, p, q, r	δ_{yaw}, PF, AMT	β_{dem}	9th

Table 2
Desired eigenvector specification elements

Element	Required effect of the state
0	no effect in the mode
1	dominant in the mode
x	unspecified: allows the unconstrained influence of the element in the mode

inputs tends to be much less than the number of states hence it is only possible to define a desired eigenvector in general which consists of the elements given in Table 2.

The feedback matrix is calculated by Equation (37):

$$\mathbf{K} = \mathbf{Z_B^{-1}U_0^T(V\Lambda - AV)V^{-1}} \quad \ldots (37)$$

where $\mathbf{Z_B}$ and $\mathbf{U_0}$ are obtained via a QR decomposition of the control matrix, **B**. Hence the parameters that must be defined to calculate **K** are the state matrix **A**, the input matrix **B** (and hence $\mathbf{Z_B}$ and $\mathbf{U_0}$), desired eigenvalues $\mathbf{\Lambda}$ and the achievable eigenvectors in the modal matrix **V**.

Continuation methods allow trim points to be calculated pseudo-continuously across a parameter space. At each point the system is linearised and eigenstructure assignment is used to calculate a set of controller gains based on the linearisation. Hence, trimming and controller design are done together. Concatenation of these local gain matrices yields a controller that will provide near 'optimum' control for all trim points throughout the parameter space. By calculating the controller gains in this way, the underlying physics of the system can be retained through the bifurcation diagrams so it is possible to examine all of the states (including the controller states) at each trim point. The dynamic gain schedules are then obtained by a direct transformation from the static.

Continuation methods are the primary tool of bifurcation analysis which has been used extensively to analyse and modify aircraft dynamics[23-26]. No bifurcations will be present in this work as the SCAS will provide a single stable trim branch throughout the given parameter space, though the diagrams will still be referred to as bifurcation diagrams.

For the purposes of assessing the effectiveness of DGS control 'ideal' systems are defined as benchmarks. They are ideal because they consist of simple transfer functions that have unity gain and the same roots as the eigenstructure assigned closed-loop system.

3.2.1 ICE (v1) – q demand

Figure 5 shows the first version of the model. The demanded eigenvalue position was $-2 \pm 2i$ for the short period mode and –5.0 for the integrator mode. The actuator mode was unconstrained. The position of the short period mode – and the modes of the other versions of the model – was chosen to just satisfy Level 1 handling qualities requirements[27]. Bifurcation diagrams for this run are shown in Fig. 6 where the solid line-type means that the solution is asymptotically stable. The eigenstructure was assigned at each continuation solution point hence the trimmed system is locally asymptotically stable and there are no bifurcation points.

The continuation parameter was constrained by the available data in the lower range (i.e. no data was available for $\alpha < -5°$). The upper limit was constrained by the control power that was available to trim the aircraft – at q_{dem} = 18deg/s the rate of change of the pitch flap angle with q_{dem} is such that the actuator lower position saturation limit of –30deg would be quickly reached for a small increase in q_{dem}.

This version of the ICE has a q_{dem} CAS, so for steady states $q = q_{dem}$ (unless there is actuator saturation). These gains can therefore be implemented directly as a function of the continuation parameter, μ, (q_{dem} parameter scheduled) which as previously stated is the same as the reference input, $\bar{r}$, for all the cases considered in this work. The static gain variations that are required to maintain Level 1 handling qualities and the derived dynamic gain variations, calculated using Equation (13) and hence still satisfying the handling qualities requirements, are shown in Fig. 7. (Note that K_α and φ_α are both dimensionless). It shows the static and dynamic gains to be equal, i.e. $K_\alpha(q_{dem}) = \varphi_\alpha(\alpha)$ when $\alpha = 0$ and when $\partial\varphi_\alpha/\partial\alpha = 0$ (as expected by Equation (12)). Similarly it shows that $K_q(q_{dem}) = \varphi_q(q)$

https://doi.org/10.1017/S0001924000000932 Published online by Cambridge University Press

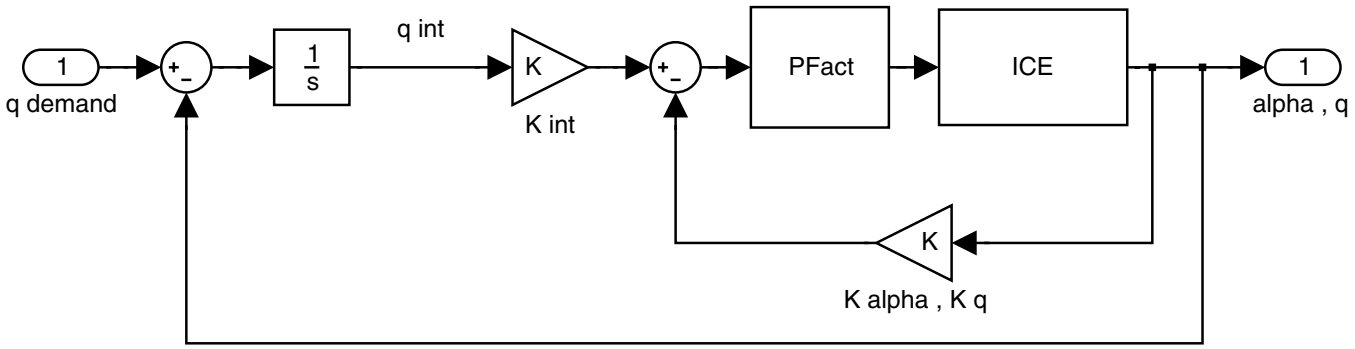


Figure 5. Block diagram of the ICE (v1).

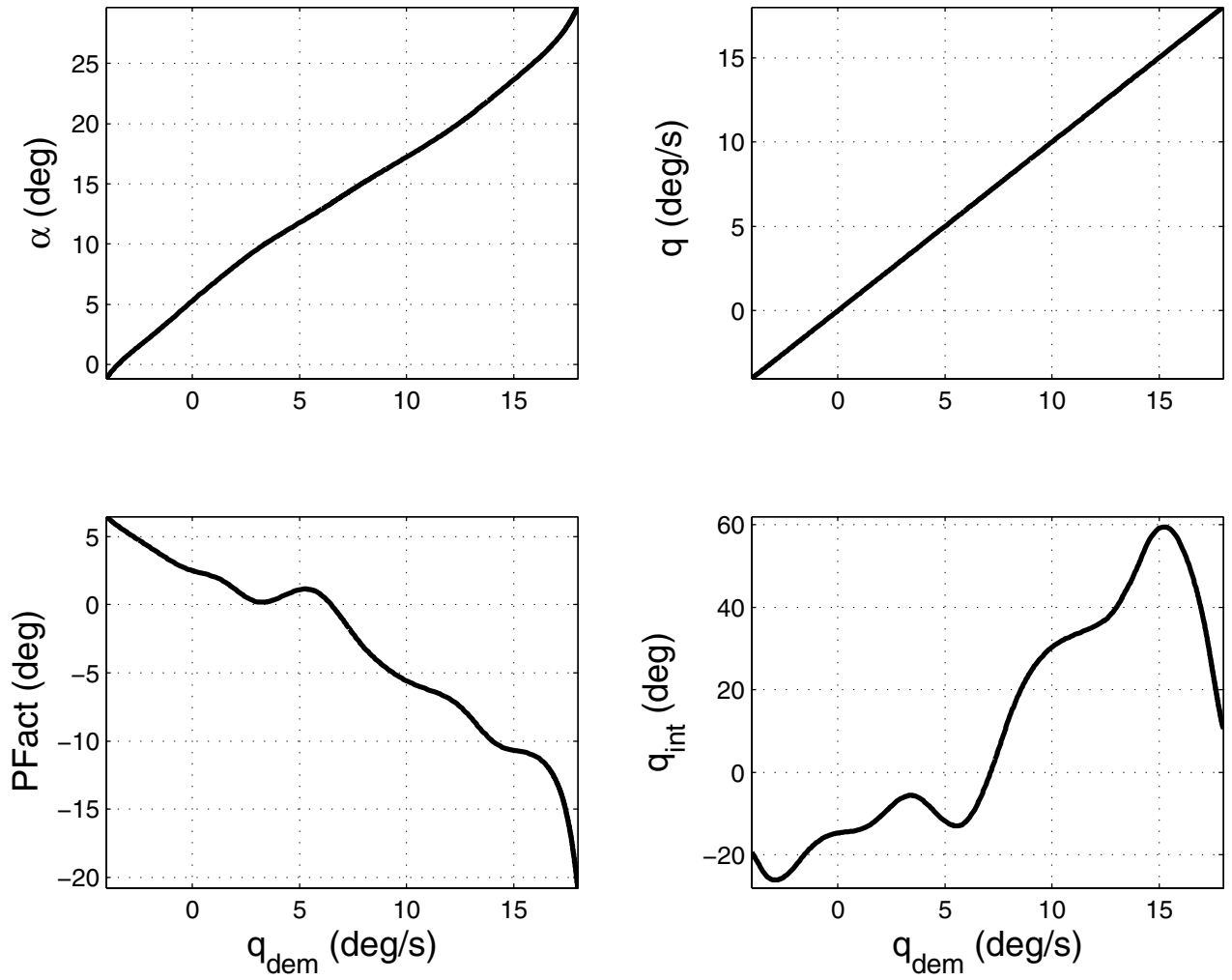


Figure 6. Bifurcation diagrams for the closed-loop ICE (v1).

https://doi.org/10.1017/S0001924000000932 Published online by Cambridge University Press

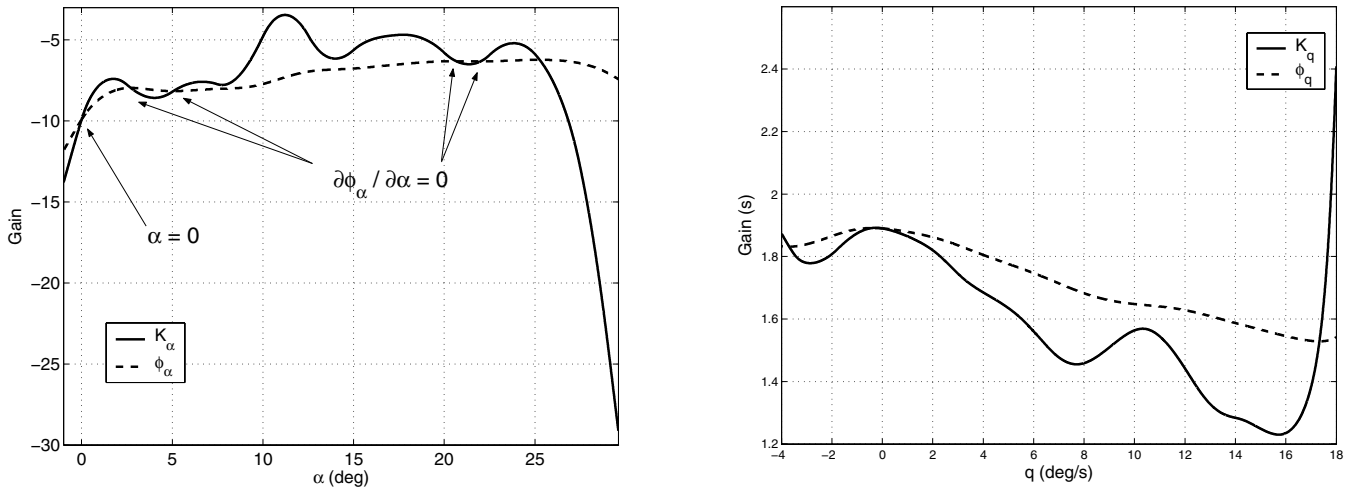


Figure 7. Transformation of K to φ for the ICE (v1).

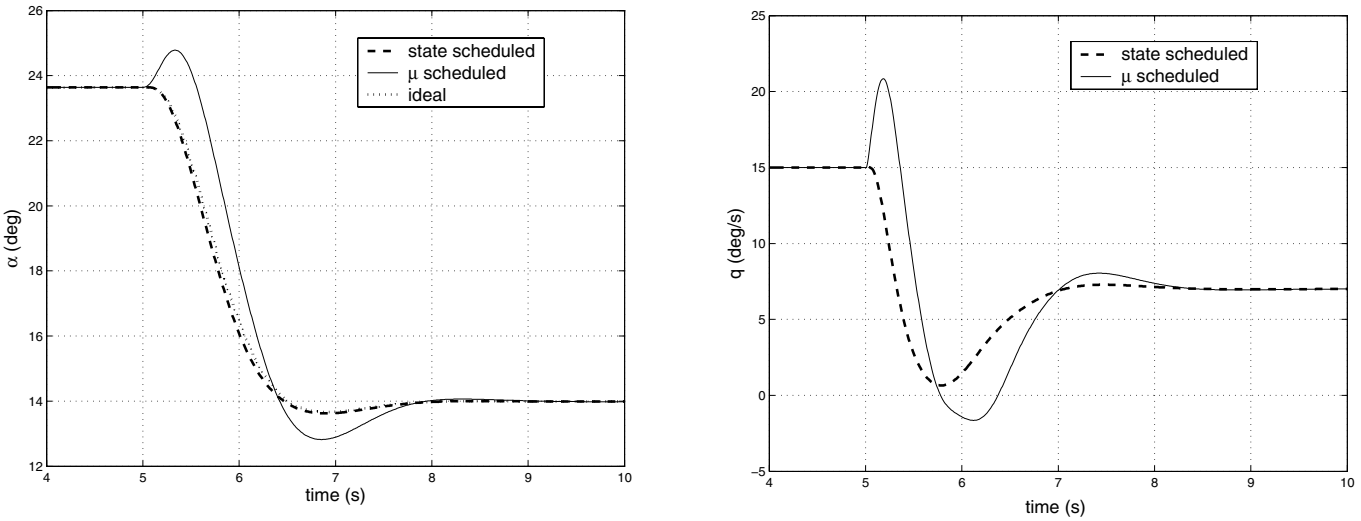


Figure 8. ICE (v1) *PFact* – response to a –8 deg/s step in q_{dem} from q = 15deg/s.

when $q = 0$ and when $\partial\varphi_q/\partial q = 0$. This actually causes one of the intersections to be hidden by the scale of the plot as $\partial\varphi_q/\partial q = 0$ just to the left of $q = 0$.

Time simulations were carried out to compare the system response when the static gains, K, were scheduled with μ to the response when the α and q dynamic gains, φ_α and φ_q respectively, were scheduled with their respective states. Due to a highly nonlinear variation of the CAS integrator gain, $K_{q_{int}}$, with the CAS integrator state, q_{int}, for simplicity initially, it remained scheduled conventionally with μ. The effect of applying so-called 'modified' transformations that allow the conversion of highly nonlinear static gain schedules (such as $K_{q_{int}}$) to dynamic ones will be shown in Section 3.2.3.

Figures 8 and 9 show the response to a fairly large (rapid) step input of –8deg/s in q_{dem} (from an initial q = 15deg/s). The ideal response was found to be almost indistinguishable from the DGS response for the plotted scale.

The magnitude and initial value of the step in Figs 8 and 9 was chosen to highlight a problem of scheduling gains with the input parameter (which could equate to stick position for a manned aircraft). When the step was applied in q_{dem} at t = 5 s the μ-scheduled system actuator response initially moved in the wrong direction. When relatively large steps in rapidly varying states (such as α or q) are demanded then the gain being applied to a point in state-space is far away from the point where the gain is optimum†. Hence when the step is applied there is an instant change in each static input-scheduled gain resulting in a large instantaneous negative signal being sent to the actuator. In fact, this signal is so large that the actuator lower position limit of –30 deg is almost saturated. This is the reason why the pitch rate response to the q_{dem} signal initially goes in the opposite direction to that which is required.

However, for the case with the state-scheduled controller the initial movement in the wrong direction is tiny (and indistin-

† Optimum is defined as a system that just satisfies Level 1 handling qualities requirements in this case though it is likely that a UCAV control system would be constrained by other factors.

https://doi.org/10.1017/S0001924000000932 Published online by Cambridge University Press

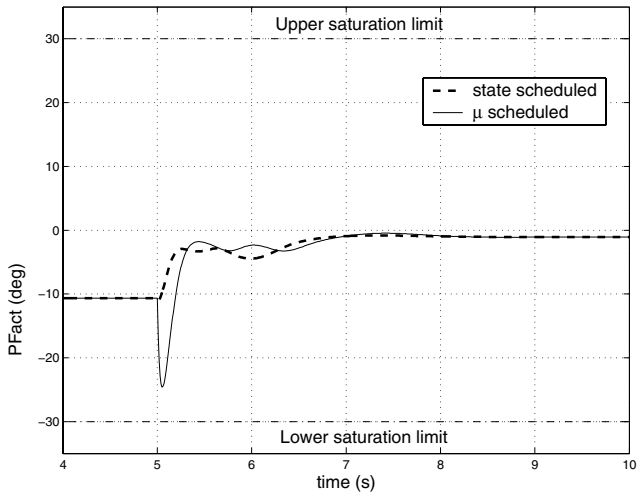


Figure 9. ICE (v1) *PFact* – response to a –8 deg/s step in q_{dem} from q = 15deg/s.

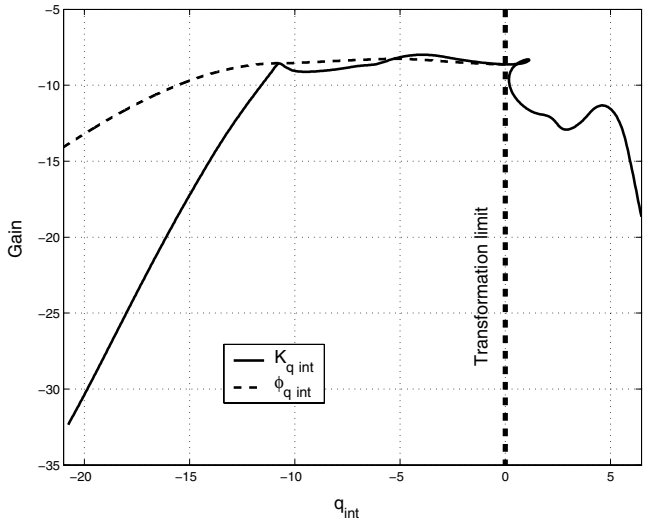


Figure 10. Transformation of K_{qint} to φ_{qint} for $q_{int} < 0$.

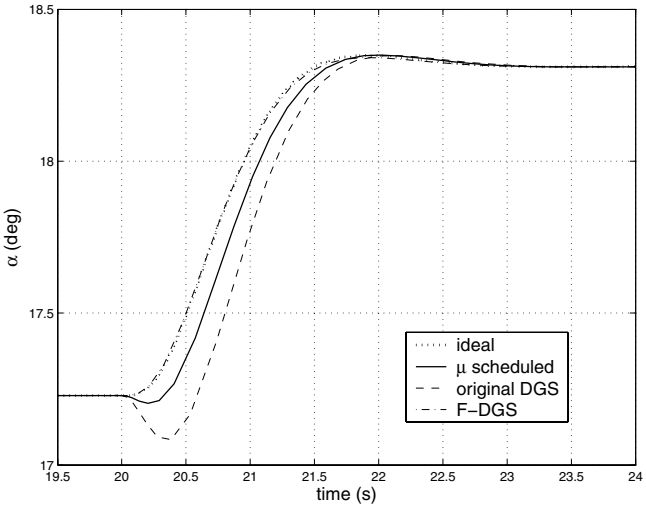


Figure 11. A comparison of the various scheduled system responses with the ideal response.

guishable for the plotted scale) because there is only a slight instant change in the feedback gains as they are now a function of the state and not the demand. The scheduling value will therefore evolve rather than step. The only initial movement is due to the CAS integrator gain (which is still scheduled with μ). The smaller movement is also due to the magnitude of the gain being reduced as a result of the transformation from K to φ. Actuator position limit saturation is no longer a problem.

In Fig. 8 the state-scheduled controller gives a near-perfect response. This is because the gain being applied is always very close to the optimum as it is being scheduled according to the system position in state-space. This is helped by the smoother variation in gains that resulted from the transformation process. The μ-scheduled system is, in contrast, evolving from one trim point (with a particular set of gains) to another trim point, and is doing so at a different (but constant) set of gains. Differences between the state-scheduled and ideal responses can be attributed to the CAS integrator gain still being μ-scheduled and the movement of the actuator pole, which was not part of the eigenstructure assignment process.

Therefore, one of the main advantages of this method of gain scheduling is for rapid manoeuvring flight where it has been shown that scheduling with a fast-varying state rather than with the input parameter gives a predictable response that is far closer to the optimum.

3.2.2 Transfer function analysis

The open-loop transfer function $q(s)/u(s)$ at the trim condition corresponding to q = 15deg/s is shown in Equation (38) where u is the input signal to the pitch flap actuator in this subsection. Hence the system is stable with an actuator pole at s = –30 and a short period mode with a damping ratio of 0·505 and an undamped natural frequency of 1·77 rad/s.

$$\frac{q(s)}{u(s)} = \frac{-141 \cdot 2(s + 0 \cdot 74)}{(s+30)(s^2 + 1 \cdot 79s + 3 \cdot 14)} \quad \ldots (38)$$

The closed-loop transfer function at the $q_{dem} = q$ = 15deg/s trim point with static gain scheduled control is given in Equation (39). The full state feedback has moved the system poles to the positions that were requested by the eigenstructure assignment algorithm (short period at $s = -2 \pm 2i$, integrator at s = –5 and actuator unconstrained).

$$\frac{q(s)}{q_{dem}(s)} = \frac{-52 \cdot 6(s - 23 \cdot 9)(s + 0 \cdot 7)}{(s^2 + 4s + 8)(s+5)(s+22)} \quad \ldots (39)$$

The equivalent closed-loop transfer function with dynamic gain scheduled control is given in Equation (40). Hence although the stability is unchanged the dynamic gain schedule has changed the numerator of this equivalent linearisation. These transfer functions suggest that a step away from this point would yield a far superior response characteristic in the dynamic gain scheduled case due to the zero dynamics being in the left hand side of the s-plane (the static gain scheduled case being non-minimum phase). This would indeed be true but the actual case of the non-linear system is more complex as the gains are calculated from a pseudo-continuous highly non-linear set of linearisations (each having different zero dynamics).

$$\frac{q(s)}{q_{dem}(s)} = \frac{237 \cdot 2(s + 5 \cdot 3)(s + 0 \cdot 7)}{(s^2 + 4s + 8)(s+5)(s+22)} \quad \ldots (40)$$

https://doi.org/10.1017/S0001924000000932 Published online by Cambridge University Press

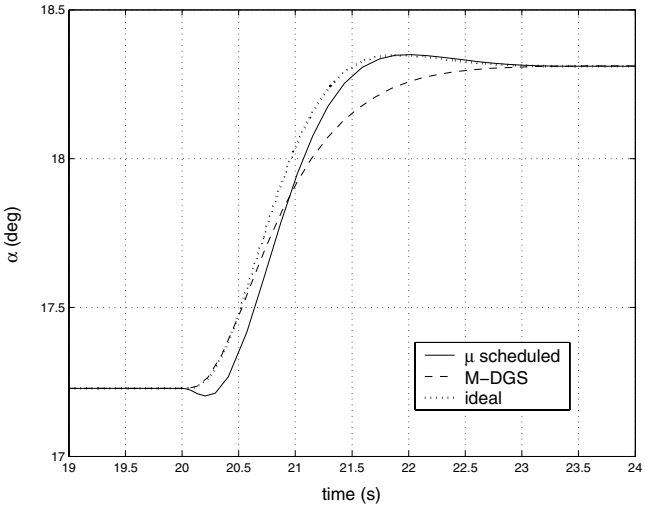


Figure 12. A comparison of the modified dynamic scheduled system response with the μ-scheduled and ideal responses.

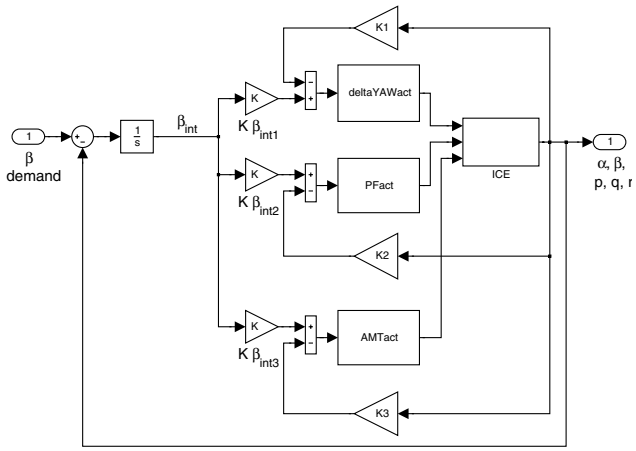


Figure 13. Block diagram for the ICE (v2).

3.2.3 Transformation of K_{qint} to φ_{qint}

Figure 10 shows the variation of the CAS integrator gain, $K_{q_{int}}$, with the CAS integrator state, q_{int}, over the region defined by the continuation parameter. (Note that the gains are dimensionless.)

Transformation of the static gain schedule, $K_{q_{int}}$, to a dynamic gain schedule, $\varphi_{q_{int}}$, across the entire range was therefore difficult, due to the multi-valued nature of $K_{q_{int}}$ for $0 < q_{int} < 1$. (This occurred due to the open-loop fold bifurcations shown in Fig. 2.) However, to test the theory the schedule was transformed only for $q_{int} < 0$ as shown in Fig. 10.

Extending the DGS system to include $\varphi_{q_{int}}$ was shown to make the ideal and actual responses virtually identical. The response to a step input of q_{dem} = 1deg/s from an initial 10deg/s is given in Fig. 11 where it is also compared to the μ-scheduled response, the original state-scheduled response (i.e. using φ_α, φ_q and $K_{q_{int}}$) and the 'ideal' response. (This particular test step input was chosen as it corresponds to a trimmed q location that is well to the left of the 'Transformation limit' line in Fig. 10, hence reducing the chances of encroaching into the multi-valued region just to the other side of it during the simulation.) Any system that transforms all of its static gain schedules to dynamic ones, without the need to transform using a state other than the feedback state, will henceforth be referred to as a full dynamic gain schedule (F-DGS) system.

Differences between the F-DGS and the ideal response are due to the movement of the actuator pole as a result of the eigenstructure assignment process – the actual position of the pole is near –22 (on the real axis of the s-plane) for the simulated region in Fig. 11.

As $K_{q_{int}}$ could not be converted to $\varphi_{q_{int}}$ over the entire range of q_{dem} the following set of 'modified' transformations (see Section 2.3) was then implemented instead:

$$
\begin{aligned}
K_\alpha(\mu) &= \varphi_\alpha(\alpha) + \left(\frac{\partial \varphi_\alpha}{\partial \alpha}\alpha\right) \\
K_q(\mu) &= \varphi_q(q) + \left(\frac{\partial \varphi_q}{\partial q}q\right) + \left(\frac{\partial \varphi_{q_{\text{int}}}}{\partial q}q_{\text{int}}\right) \qquad \ldots (41) \\
K_{q_{\text{int}}}(\mu) &= \varphi_{q_{\text{int}}}(q)
\end{aligned}
$$

Hence the integrator gain was dynamic scheduled with trimmed q instead of q_{int} since it remains single-valued throughout the required range. The effect of this transformation is shown in Fig. 12 where the α-response to the same step input in q_{dem} of 1deg/s (as in Fig. 11), using this modified dynamic and conventional μ-scheduling, are compared. Any state-scheduled system response where the dynamic gains have been obtained using a modified transformation will be referred to as a modified dynamic gain schedule (M-DGS) in all subsequent figures. Hence the response is better using the M-DGS system than the μ-scheduled system as there is no initial movement in the wrong direction. It is worse than the F-DGS system response but it has already been stated that it is not always possible for this kind of schedule to be attained.

Hence, although the M-DGS system has the correct eigenstructure, its responses (although better than the μ-scheduled system) are still not close to the F-DGS system and hence the 'ideal' responses. This happens because all gains are calculated at trim points. Discrepancies arise when the scheduling state differs significantly from its trim value. This is most likely to be important when using the unsmoothed static gain variation. Hence the F-DGS case is most desirable as all the schedules are transformed.

3.2.4 ICE (v2) – β demand

Figure 13 shows the second version (v2) of the model to be tested where K_i is a vector of gains ($K_{\alpha i}$, $K_{\beta i}$, K_{pi}, K_{qi}, K_{ri}) that is multiplied by the feedback state vector.

As the all-moving tip (AMT), sometimes referred to as a 'wingeron', is an unusual control effector a brief description of its characteristics (taken from Ref. 10) will first be given.

It is mainly used to create drag at the wing tip to yaw the aircraft but it also creates nonlinear roll and pitch forces. The rolling moment actually reverses direction as the angle of incidence changes. At low incidence, below 5-10°, it produces rolling moments in the conventional sense, i.e. if the right tip deflects trailing edge down, the aircraft will roll to the left. However at higher incidence, above 5-10°, the same right wingtip deflection will make the aircraft roll right because the flow separates rapidly and destroys lift. This also produces a stronger yawing moment.

The yaw control is hence produced by creating drag at the wing tips. Wind tunnel experience has indicated that the AMT is an excellent source of yaw control power. Yaw control magnitudes at large deflections are on the order of that produced by an F-16 rudder.

The AMT yaw power is invariant to windward sideslip and suffers only slight degradation with leeward sideslip for all angles of

https://doi.org/10.1017/S0001924000000932 Published online by Cambridge University Press

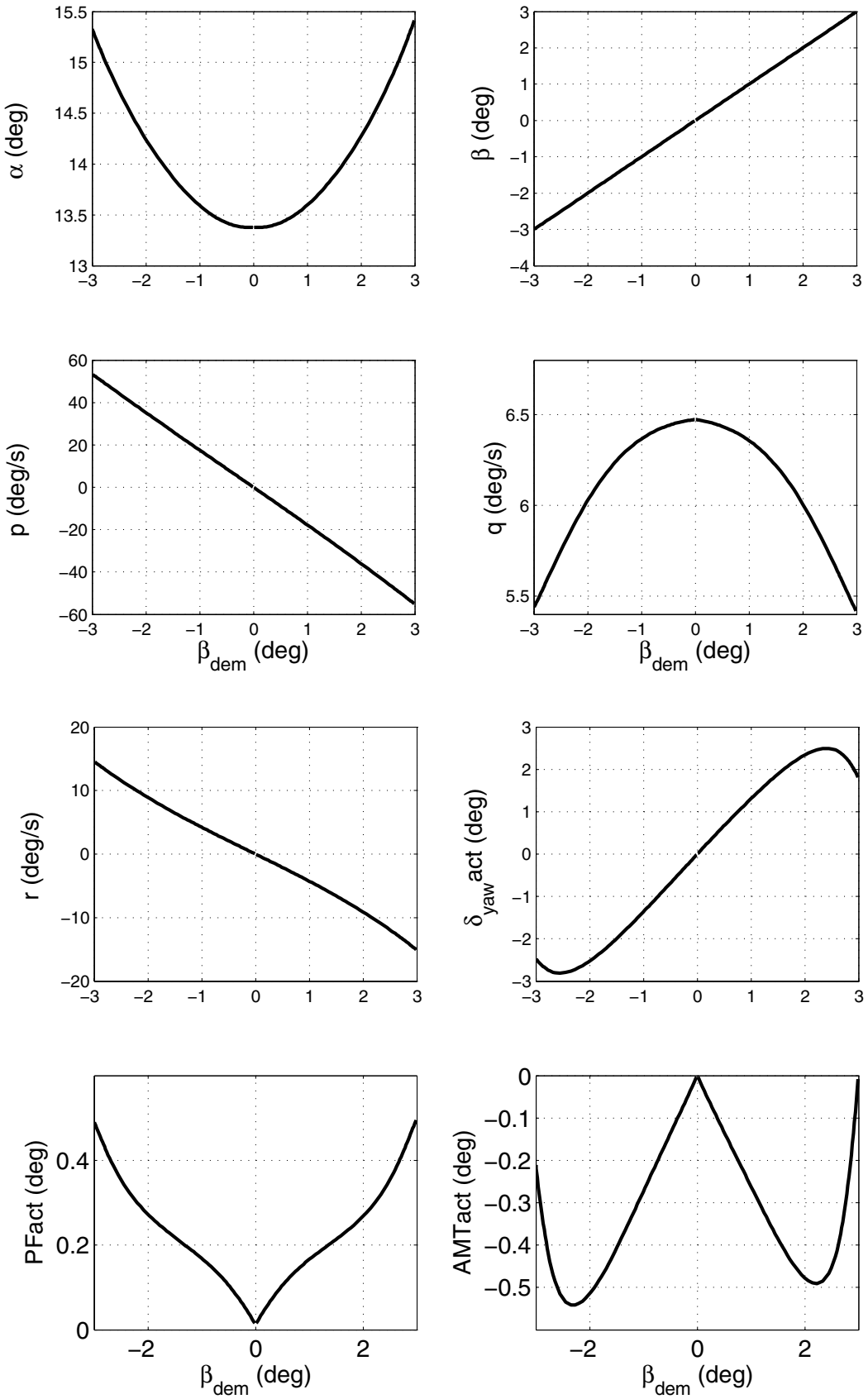


Figure 14. Bifurcation diagrams for the closed-loop ICE (v2).

https://doi.org/10.1017/S0001924000000932 Published online by Cambridge University Press

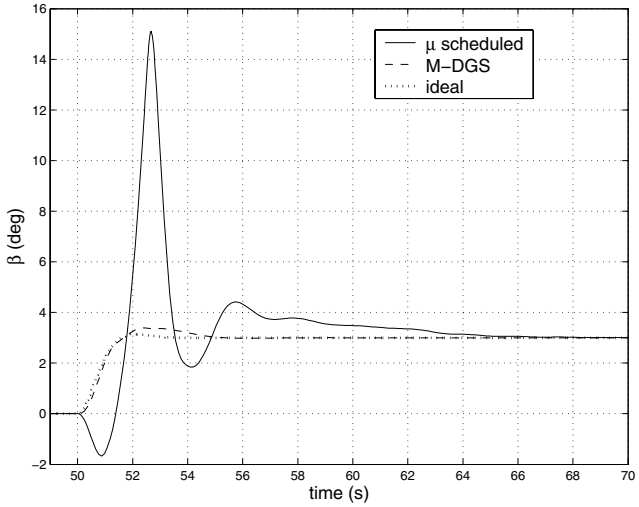


Figure 15. Comparison of the static and M-DGS system response in β to a step input in β_{dem} of 3deg.

incidence. This is a very desirable characteristic hence the AMT was intended to be primarily used to counter sideslip and provide directional control for the aircraft. It was also designed, in part, so that it could be constrained to move only in one direction in order to reduce its radar cross section. Hence only negative effector movements (i.e. trailing edge up) will be allowed in this example.

The five aircraft dynamic modes were assigned in order to satisfy Level 1 handling qualities with the short period at $-2{\cdot}0 \pm 2{\cdot}0i$, the Dutch roll at $-1{\cdot}5 \pm 1{\cdot}5i$ and the roll subsidence mode at $-3{\cdot}0$. The CAS integrator mode was placed at $-2{\cdot}5$ with its position once again being somewhat of a compromise between the desire for a pole far away from the imaginary axis and the need to keep the gains as small as possible. Bifurcation diagrams for a constrained run ($-3° \leq \beta_{dem} \leq 3°$) are shown in Fig. 14. The β_{dem} limits emanated from the requirement that the AMTs should be constrained so that they could only move in one direction. Therefore, the limits represent the maximum achievable β-trim that can be obtained using this combination of effectors.

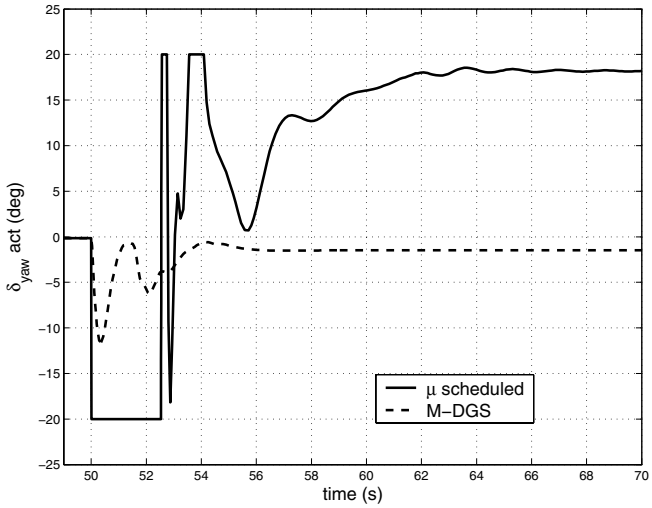
The eigenstructure assignment of the first two versions of the model was fairly minimal (i.e the desired eigenvectors had few constraints). However, for this run the desired eigenstructure was specified to a much greater extent in order to minimise the interaction of the longitudinal and lateral aircraft modes. The desired eigenvectors, ν_t^d, that were used in the eigenstructure assignment process (see Section 3.2) are shown in Equation (42) where ν_1^d and ν_2^d assigned the short period, ν_3^d and ν_4^d assigned the Dutch roll, ν_5^d assigned the roll subsidence and ν_6^d assigned the CAS integrator. The state order was (α, β, p, q, r, $\delta_{yaw}act$, *PFact*, *AMTact*, β_{int}).

$$\boldsymbol{v}_1^d = \begin{bmatrix} 1 \\ 0 \\ 0 \\ x \\ 0 \\ 0 \\ x \\ 0 \\ 0 \end{bmatrix} \quad \boldsymbol{v}_2^d = \begin{bmatrix} x \\ 0 \\ 0 \\ 1 \\ 0 \\ 0 \\ x \\ 0 \\ 0 \end{bmatrix} \quad \boldsymbol{v}_3^d = \begin{bmatrix} 0 \\ x \\ 0 \\ 0 \\ 1 \\ 0 \\ 0 \\ x \\ x \end{bmatrix} \quad \boldsymbol{v}_4^d = \begin{bmatrix} 0 \\ 1 \\ 0 \\ 0 \\ x \\ 0 \\ 0 \\ x \\ x \end{bmatrix} \quad \boldsymbol{v}_5^d = \begin{bmatrix} 0 \\ x \\ 1 \\ 0 \\ x \\ x \\ 0 \\ x \\ x \end{bmatrix} \quad \boldsymbol{v}_6^d = \begin{bmatrix} 0 \\ 1 \\ x \\ 0 \\ x \\ x \\ 0 \\ x \\ 1 \end{bmatrix} \quad \ldots (42)$$

The static gains were converted to dynamic gains using the following set of modified transformations:

$$\begin{aligned} K_\alpha &= \varphi_\alpha(\beta) \\ K_\beta &= \varphi_\beta(\beta) + \left(\frac{\partial \varphi_\beta}{\partial \beta}\beta\right) + \left(\frac{\partial \varphi_\alpha}{\partial \beta}\alpha\right) + \left(\frac{\partial \varphi_p}{\partial \beta}p\right) \\ &\quad + \left(\frac{\partial \varphi_q}{\partial \beta}q\right) + \left(\frac{\partial \varphi_r}{\partial \beta}r\right) + \left(\frac{\partial \varphi_{\beta_{\text{int}}}}{\partial \beta}\beta_{\text{int}}\right) \\ K_p &= \varphi_p(\beta) \\ K_q &= \varphi_q(\beta) \\ K_r &= \varphi_r(\beta) \\ K_{\beta_{\text{int}}} &= \varphi_{\beta_{\text{int}}}(\beta) \end{aligned} \quad \ldots (43)$$

A simulation was carried out to compare the β_{dem} -scheduled static gain system with the M-DGS system. The static system response in β and the control effector actuators to a step input in β_{dem} of 3deg is shown in Figs 15 to 17.



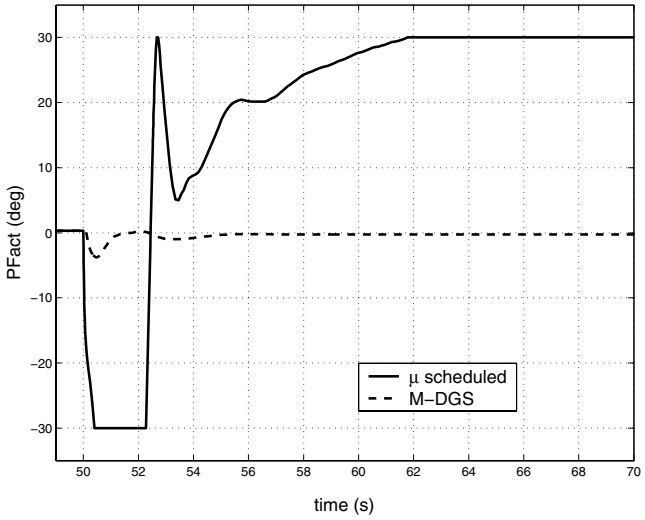


Figure 16. Comparison of the static and M-DGS system response in $\delta_{yaw}act$ and *PFact* to a step input in β_{dem} of 3deg.

https://doi.org/10.1017/S0001924000000932 Published online by Cambridge University Press

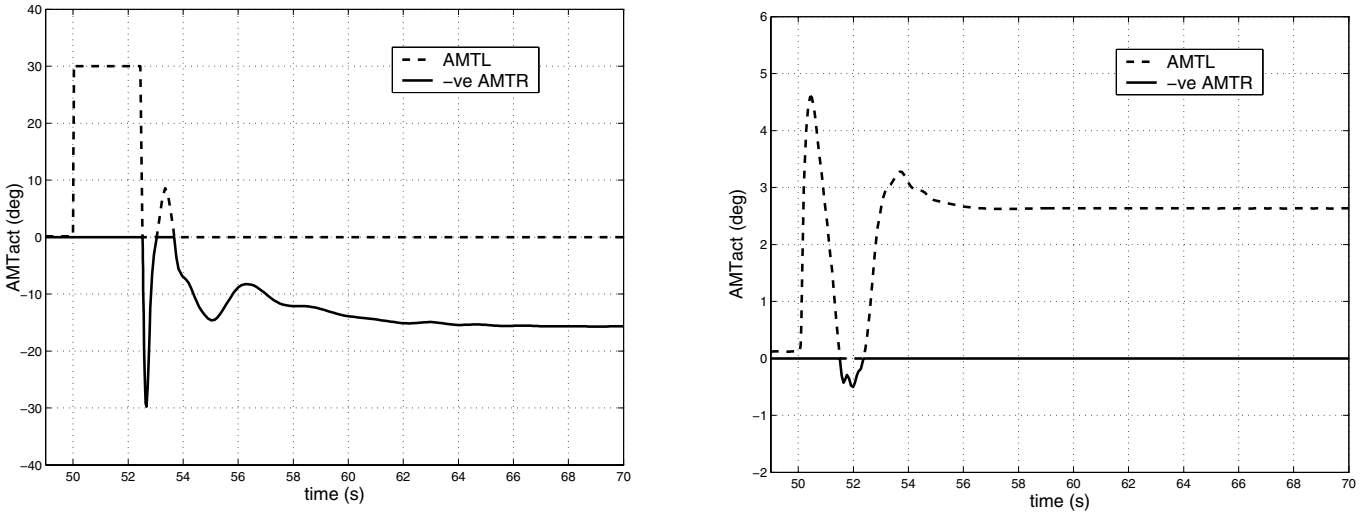


Figure 17. Comparison of the static and M-DGS system response in *AMTact* to a step input in β_{dem} of 3deg.

Each is compared to the M-DGS system response and Fig. 15 is also compared to the 'ideal' response. (The right AMT (AMTR) actuator position was multiplied by –1 before it was plotted so that the 'co-operation' of the left AMT (AMTL) with AMTR during the step response could be more easily visualised.) Hence the M-DGS system response in β is close to the 'ideal' response and is vastly superior to the μ-scheduled system response which shows large regions of saturation in each actuator.

4.0 CONCLUSIONS AND FUTURE WORK

In this paper a method for scheduling gains against rapidly changing states has been applied to a UCAV model. The dynamic gains were determined directly by applying a transformation to static gain schedules which were themselves calculated quasi-continuously from within a continuation design framework using eigenstructure assignment.

- The method was shown to vastly improve the transient response for both longitudinal and longitudinal/lateral versions of the model when stepping between trim conditions.
- The problem of control surface position limit saturation has also been shown to be less likely when a DGS is used as the magnitude of the gains are generally smaller than the original static gains as a result of the transformation process.
- DGS transformation was also found to have the additional benefit of smoothing the highly nonlinear gain variation that results when a very precise control law design method such as eigenstructure assignment is used. Future work will involve the application of other design tools such as LQR and the determination of whether this advantage is retained when the static gain variations are smoother.
- The original work on DGS[1] was only applicable to reduced order systems. This paper has advanced the method with the addition of modified static-to-dynamic gain schedule transformations. This allowed its extension to a longitudinal/lateral aircraft model by proposing a means of designing dynamic gain schedules when multi-valued behaviour arises in non-linear systems (i.e. several trimmed gain values corresponding to a single state value). Future work will include its application to 'real' (i.e. unconstrained) aircraft models and practical testing of the control law in a wind tunnel.
- Future work will also involve the scheduling of the dynamic gains with several states and the inevitable comparison with Nonlinear Dynamic Inversion (NDI)[28,29] that such an implementation will require.
- Consideration of the state signals that can be measured will necessitate a study of output rather than full state feedback controllers.

ACKNOWLEDGEMENTS

The supply of data for the ICE 101-TV model by the Air Force Research Laboratory at Wright-Patterson Air Force Base is gratefully acknowledged.

REFERENCES

1. RICHARDSON, T.S., DAVISON, P.M., LOWENBERG, M.H. and DI BERNARDO, M. Control of nonlinear aircraft models using dynamic state-feedback gain scheduling, Proceedings of the AIAA Atmospheric Flight Mechanics Conference, AIAA 2003-5503.
2. REICHERT, R.T. Dynamic scheduling of modern-robust-control autopilot designs for missiles, *IEEE Control Systems Magazine*, 1992, **12**, (5), pp 35-42.
3. REICHERT, R.T. Gain scheduling for *h*-infinity controllers: A flight control example 1992, Technical report, John Hopkins University, Baltimore, MD.
4. SHAHRUZ, S.M. and BEHTASH, S. Design of controllers for linear parameter-varying systems by the gain-scheduling technique, *J Math Analysis and Applications*, 1992, **168**, (1), pp 195-217.
5. RUGH, W.J. and SHAMMA, J.S. Research on gain scheduling, *Automatica*, 2000, **36**, (10), pp 1401-1425.
6. SHAMMA, J.S. Special issue on gain scheduling, *Int J Robust and Nonlinear Control*, 2002, **12**, (9).
7. SHAMMA, J.S. and ATHANS, M. Analysis of gain-scheduled control for nonlinear plants, *IEEE Transactions on Automatic Control*, 1998, **35**, (8), pp 898-907.
8. STILWELL, D.J. and RUGH, W.J. Stability preserving interpolation methods for the synthesis of gain scheduled controllers, *Automatica*, 2000, **36**, pp 665-671.
9. LEITH, D.J. and LEITHEAD, W.E. Survey of gain-scheduling analysis & design, *Int J of Control*, 2000, **73**, (11), pp 1001-1025.
10. DORSETT, K.M. and MEHL, D.R. Innovative control effectors (ICE), January 1996, Wright Laboratories, Wright-Patterson AFB, OH, WL-TR-96-3043.

https://doi.org/10.1017/S0001924000000932 Published online by Cambridge University Press

11. DORSETT, K.M. ET AL Innovative control effectors (ICE) Phase II, July 1997, Wright Laboratories, Wright-Patterson AFB, OH, WL-TR-97-3059.
12. MASEY, J. *Unmanned Vehicles Handbook 2005*, 2004, The Shephard Press.
13. LOWENBERG, M.H. and RICHARDSON, T.S. The continuation design framework for nonlinear aircraft control, 2001, Proceedings of AIAA Guidance, Navigation and Control Conference, AIAA-2001-4100.
14. JONES, C.D.C., RICHARDSON, T.S. and LOWENBERG, M.H. Dynamic state-feedback gain scheduled control of the ICE 101-TV, 2004, Proceedings of AIAA Guidance, Navigation and Control Conference, AIAA 2004-4754.
15. ANDRY, A.N., SHAPIRO, E.Y. and CHUNG, J.C. Eigenstructure assignment for linear systems, September 1983, IEEE Transactions on Aerospace and Electronic Systems, AES, **19**, (5), pp 711-728.
16. SOBEL, K.M., SHAPIRO, E.Y. and ANDRY, A.N. Eigenstructure assignment, *Int J of Control*, 1994, **59**, (1), pp 13-37.
17. GIBSON, L., NICHOLS, N.K. and LITTLEBOY, D.M. Closed loop design for a simple nonlinear aircraft model using eigenstructure assignment, 1997, Proceedings of AIAA Guidance, Navigation and Control Conference, AIAA-97-3779.
18. RICHARDSON, T.S. Continuation Methods Applied to Nonlinear Flight Dynamics and Control, 2002, PhD thesis, University of Bristol.
19. HYDE, R.A. The Application of Robust Control to VSTOL Aircraft, August 1991, PhD Thesis, University of Cambridge.
20. TISCHLER, M.B., LEE, J.A. and COLBOURNE, J.D. Optimisation and comparison of alternative flight control system design methods using a common set of handling-qualities criteria, 2001, Proceedings of the AIAA Guidance, Navigation and Control Conference, AIAA 2001-4266.
21. NELSON, R.C. *Flight Stability and Automatic Control*, 1998, McGraw-Hill.
22. DOEDEL, E.J. *AUTO 97 – Continuation and Bifurcation Software for Ordinary Differential Equations*, 1998.
23. CARROL, J.V. and MEHRA, R.K. Bifurcation analysis of nonlinear aircraft dynamics, *J Guidance, Control and Dynamics*, September-October 1982, **5**, (5), pp 529-536.
24. AVANZINI, G. and DE MATTEIS, G. Bifurcation analysis of a highly augmented aircraft model, 1996, Proceedings of the AIAA Atmospheric Flight Mechanics Conference, AIAA-96-3367-CP.
25. JAHNKE, C.C. and CULICK, F.F.C. Application of bifurcation theory to the high-angle-of-attack dynamics of the F-14, *J Aircr*, January-February 1994, **31**, (1), pp 26-34.
26. LOWENBERG, M.H. Application of Bifurcation Analysis to Multiple Attractor Flight Dynamics, August 1998, PhD Thesis, University of Bristol.
27. HODGKINSON, J. *Aircraft Handling Qualities*, American Institute of Aeronautics and Astronautics Press.
28. SMITH, P.R. Functional control law design using exact nonlinear dynamic inversion, 1994, AIAA Atmospheric Flight Mechanics Conference Technical Papers, AIAA-94-3516-CP, pp 481-489.
29. SCHUMACHER, C. and KHARGONEKAR, P.P. Missile autopilot designs using H8 control with gain scheduling and dynamic inversion, *J Guidance, Control, and Dynamics*, March-April 1998, **21**, (2).

https://doi.org/10.1017/S0001924000000932 Published online by Cambridge University Press